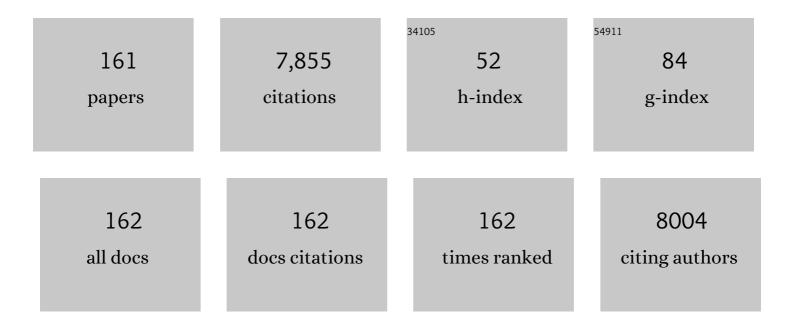
List of Publications by Year in descending order

Source: https://exaly.com/author-pdf/3581723/publications.pdf Version: 2024-02-01



#	Article	IF	CITATIONS
1	Characterization of a novel microhotplate for application in a silicon-based nanofilm gas sensor. Instrumentation Science and Technology, 2023, 51, 45-58.	1.8	1
2	MoS <sub>2</sub> -Templated Porous Hollow MoO <sub>3</sub> Microspheres for Highly Selective Ammonia Sensing via a Lewis Acid-Base Interaction. IEEE Transactions on Industrial Electronics, 2022, 69, 960-970.	7.9	85
3	Preparation of SnO2/SiO2 nanocomposites by sol-gel method for enhancing the gas sensing performance to triethylamine. Journal of Alloys and Compounds, 2022, 893, 162189.	5.5	34
4	Detection of four alcohol homologue gases by ZnO gas sensor in dynamic interval temperature modulation mode. Sensors and Actuators B: Chemical, 2022, 350, 130867.	7.8	76
5	Rational design of CuO/In2O3 heterostructures with flower-like structures for low temperature detection of formaldehyde. Journal of Alloys and Compounds, 2022, 896, 162959.	5.5	8
6	NiO-functionalized In2O3 flower-like structures with enhanced trimethylamine gas sensing performance. Applied Surface Science, 2022, 577, 151877.	6.1	33
7	Humidity sensing and temperature response performance of polymer gel cold-spliced optical fiber Fabry-Perot interferometer. Optical Fiber Technology, 2022, 68, 102823.	2.7	6
8	Phosphorus-doped porous perovskite LaFe1-xPxO3-l̂´ nanosheets with rich surface oxygen vacancies for ppb level acetone sensing at low temperature. Chemical Engineering Journal, 2022, 431, 134280.	12.7	66
9	Formic acid gas sensor based on coreless optical fiber coated by molybdenum disulfide nanosheet. Journal of Alloys and Compounds, 2022, 896, 163063.	5.5	10
10	Optimal construction and gas sensing properties of SnO2@TiO2 heterostructured nanorods. Sensors and Actuators B: Chemical, 2022, 355, 131261.	7.8	14
11	Investigation on Butanone Sensing Properties of ZnO Sensor Under Different Calcination Temperature. IEEE Sensors Journal, 2022, 22, 25-32.	4.7	10
12	Research Progress on Coating of Sensitive Materials for Micro-Hotplate Gas Sensor. Micromachines, 2022, 13, 491.	2.9	7
13	A fiber-optic formic acid gas sensor based on molybdenum disulfide nanosheets and chitosan works at room temperature. Optics and Laser Technology, 2022, 150, 107975.	4.6	14
14	A high-capacity and reversible patient data hiding scheme for telemedicine. Biomedical Signal Processing and Control, 2022, 76, 103706.	5.7	10
15	Preparation of p-LaFeOâ, <i>f</i> /n-Feâ,,Oâ, <i>f</i> Heterojunction Composites by One-Step Hydrothermal Method and Gas Sensing Properties for Acetone. IEEE Transactions on Instrumentation and Measurement, 2022, 71, 1-9.	4.7	7
16	A highly selective and fast-responding triethylamine sensor based on Mo-SnO2 nanomaterials. Sensors and Actuators Reports, 2022, 4, 100106.	4.4	2
17	Novel combined waveform temperature modulation method of NiO-In2O3 based gas sensor for measuring and identifying VOC gases. Journal of Alloys and Compounds, 2022, 918, 165510.	5.5	20
18	UV-Light Assisted High-Performance n-Propanol Sensor Based on Rod-Like Co-Modified ZnO at Room Temperature. IEEE Sensors Journal, 2022, 22, 13882-13890.	4.7	3

#	Article	IF	CITATIONS
19	Metal Oxide Semiconductor Sensors for Triethylamine Detection: Sensing Performance and Improvements. Chemosensors, 2022, 10, 231.	3.6	27
20	Exposure Surface Active Sites of Perovskiteâ€Type LaFeO <sub>3</sub> Gas Sensors by Selectively Dissolving La Cations for Enhancing Gas Sensing Properties to Acetone. Advanced Materials Technologies, 2022, 7, .	5.8	19
21	Dynamic Measurement of VOCs with Multiple Characteristic Peaks Based on Temperature Modulation of ZnO Gas Sensor. Chemosensors, 2022, 10, 226.	3.6	2
22	Dynamic Temperature Modulation Measurement of VOC Gases Based on SnO <sub>2</sub> Gas Sensor. IEEE Sensors Journal, 2022, 22, 14708-14716.	4.7	19
23	Preparation of NiO-In <sub>2</sub> O <sub>3</sub> Ordered Porous Thin Film Materials With Enhanced n-Propanol Gas Sensing Properties. IEEE Sensors Journal, 2022, 22, 15716-15723.	4.7	7
24	Ppb-Level Triethylamine Gas Sensors Based on Palladium Nanoparticles Modified Flower-Like In <sub>2</sub> O <sub>3</sub> Grown on rGO Nanosheets Operating at Low Temperature. IEEE Transactions on Instrumentation and Measurement, 2022, 71, 1-9.	4.7	12
25	Structure design and application of hollow core microstructured optical fiber gas sensor: A review. Optics and Laser Technology, 2021, 135, 106658.	4.6	73
26	P-n junctions based on CuO-decorated ZnO nanowires for ethanol sensing application. Applied Surface Science, 2021, 538, 148140.	6.1	66
27	The investigation and DFT calculation on the gas sensing properties of nanostructured SnO2. Microelectronic Engineering, 2021, 236, 111469.	2.4	13
28	Room-Temperature NH <sub>3</sub> Sensors Based on Boron-Doped Graphene Oxide: Enhanced Sensing Performance by B-N Covalent Interaction. IEEE Nanotechnology Magazine, 2021, 20, 726-732.	2.0	6
29	Ppb-Level Xylene Gas Sensors Based on Co <sub>3</sub> O <sub>4</sub> Nanoparticle-Coated Reduced Graphene Oxide(rGO) Nanosheets Operating at Low Temperature. IEEE Transactions on Instrumentation and Measurement, 2021, 70, 1-10.	4.7	60
30	High Response Formic Acid Gas Sensor Based on MoS <sub>2</sub> Nanosheets. IEEE Nanotechnology Magazine, 2021, 20, 177-184.	2.0	16
31	Investigation of Mixed-Phase WS <sub>2</sub> Nanomaterials for Ammonia Gas Sensing. IEEE Sensors Journal, 2021, 21, 7268-7274.	4.7	20
32	Dynamic Measurement and Recognition Methods of SnO <sub>2</sub> Sensor to VOCs Under Zigzag-Rectangular Wave Temperature Modulation. IEEE Sensors Journal, 2021, 21, 10915-10922.	4.7	23
33	Selectively enhanced gas-sensing performance to n-butanol based on uniform CdO-decorated porous ZnO nanobelts. Sensors and Actuators B: Chemical, 2021, 334, 129667.	7.8	18
34	Strategies for Improving the Sensing Performance of Semiconductor Gas Sensors for High-Performance Formaldehyde Detection: A Review. Chemosensors, 2021, 9, 179.	3.6	28
35	Theoretical and Experimental Research on Ammonia Sensing Properties of Sulfur-Doped Graphene Oxide. Chemosensors, 2021, 9, 220.	3.6	8
36	Perovskite-structured LaCoO3 modified ZnO gas sensor and investigation on its gas sensing mechanism by first principle. Sensors and Actuators B: Chemical, 2021, 341, 130015.	7.8	138

#	Article	IF	CITATIONS
37	Highly Sensitive and Selective NH <sub>3</sub> Sensor Based on Au Nanoparticle Loaded MoO <sub>3</sub> Nanorods. IEEE Sensors Journal, 2021, 21, 18435-18442.	4.7	11
38	Research of Low-Power MEMS-Based Micro Hotplates Gas Sensor: A Review. IEEE Sensors Journal, 2021, 21, 18368-18380.	4.7	14
39	One-step synthesis of rGO/V2O5 flower-like microsphere composites with enhanced trimethylamine sensing properties. Materials Letters, 2021, 299, 130023.	2.6	8
40	The rapid SERS detection of succinylcholine chloride in human plasma is based on the high affinity between quaternary ammonium salt structures. Spectrochimica Acta - Part A: Molecular and Biomolecular Spectroscopy, 2021, 263, 120172.	3.9	1
41	Qualitative and quantitative recognition method of drug-producing chemicals based on SnO2 gas sensor with dynamic measurement and PCA weak separation. Sensors and Actuators B: Chemical, 2021, 348, 130698.	7.8	76
42	Rose-Like MoOâ,ƒ/MoSâ,,/rGO Low-Temperature Ammonia Sensors Based on Multigas Detection Methods. IEEE Transactions on Instrumentation and Measurement, 2021, 70, 1-9.	4.7	30
43	Ammonia Sensor Based on Monoclinic WO <sub>3</sub> Nanorods Operating at Room Temperature. IEEE Nanotechnology Magazine, 2021, 20, 619-626.	2.0	2
44	A Temperature-Modulated Gas Sensor Based on CdO-Decorated Porous ZnO Nanobelts for the Recognizable Detection of Ethanol, Propanol, and Isopropanol. IEEE Sensors Journal, 2021, 21, 25590-25596.	4.7	12
45	Ppb-Level Butanone Sensor Based on ZnO-TiO2-rGO Nanocomposites. Chemosensors, 2021, 9, 284.	3.6	6
46	MoO <sub>3</sub> /SnO <sub>2</sub> Nanocomposite-Based Gas Sensor for Rapid Detection of Ammonia. IEEE Transactions on Instrumentation and Measurement, 2021, 70, 1-9.	4.7	14
47	WOâ,ƒ Nanosheets/FeCoâ,"Oâ," Nanoparticles Heterostructures for Highly Sensitive and Selective Ammonia Sensors. IEEE Sensors Journal, 2021, 21, 26515-26525.	4.7	9
48	One-step synthesis and the enhanced trimethylamine sensing properties of Co3O4/SnO2 flower-like structures. Vacuum, 2020, 171, 108994.	3.5	37
49	Graphene Foam Decorated With ZnO as a Humidity Sensor. IEEE Sensors Journal, 2020, 20, 1721-1729.	4.7	28
50	Detection and Identification of Volatile Organic Compounds Based on Temperature-Modulated ZnO Sensors. IEEE Transactions on Instrumentation and Measurement, 2020, 69, 4533-4544.	4.7	104
51	Investigation of Grain Radius Dependence of Sensitivity for Porous Thin Film Semiconducting Metal Oxide Gas Sensor. IEEE Sensors Journal, 2020, 20, 4275-4282.	4.7	16
52	In-situ growth of V2O5 flower-like structures on ceramic tubes and their trimethylamine sensing properties. Chinese Chemical Letters, 2020, 31, 2133-2136.	9.0	16
53	Microscale analysis and gas sensing characteristics based on SnO2 hollow spheres. Microelectronic Engineering, 2020, 231, 111372.	2.4	12
54	Highly Sensitive Ethanol Sensor Based on Two-Dimensional Layered Mesoporous In <sub>2</sub> O <sub>3</sub> Nanosheets. IEEE Nanotechnology Magazine, 2020, 19, 486-491.	2.0	1

#	Article	IF	CITATIONS
55	Spinel-Type Materials Used for Gas Sensing: A Review. Sensors, 2020, 20, 5413.	3.8	31
56	Nanocomposites of ZnO Nanorods In-Situ Grown on Graphitic Carbon Nitride for Ethanol Sensing. IEEE Sensors Journal, 2020, 20, 11097-11104.	4.7	7
57	Ethanol Sensors Based on Porous In2O3 Nanosheet-Assembled Micro-Flowers. Sensors, 2020, 20, 3353.	3.8	16
58	Hydrogen Leakage Detectors Based on a Polymer Microfiber Decorated With Pd Nanoparticles. IEEE Sensors Journal, 2019, 19, 6736-6741.	4.7	11
59	An Efficient Base Conversion Using Variable Length Segmentation and Remainder Transfer. IEEE Signal Processing Letters, 2019, 26, 1227-1231.	3.6	2
60	Synthesis of Au Nanoparticle-Modified Spindle Shaped α-Fe <sub>2</sub> O <sub>3</sub> Nanorods and Their Gas Sensing Properties to N-Butanol. IEEE Nanotechnology Magazine, 2019, 18, 911-920.	2.0	29
61	High Response and Selectivity Ammonia Sensor Based on WO <sub>3</sub> /MoO <sub>3</sub> Porous and Hollow Microsphere. IEEE Sensors Journal, 2019, 19, 11014-11020.	4.7	11
62	ZnO-Reduced Graphene Oxide Composites Sensitized with Graphitic Carbon Nitride Nanosheets for Ethanol Sensing. ACS Applied Nano Materials, 2019, 2, 2734-2742.	5.0	84
63	InvestigationÂonÂTrimethylamineÂSensingÂPerformanceÂofÂPdOâ€DecoratedÂZnOÂFlowerâ€Like StructuresÂSynthesizedÂbyÂOne―StepAHydrothermalÂMethod. ChemistrySelect, 2019, 4, 2694-2702.	1.5	6
64	Approaches to Enhancing Gas Sensing Properties: A Review. Sensors, 2019, 19, 1495.	3.8	97
65	Sandwich-like composites of double-layer Co3O4 and reduced graphene oxide and their sensing properties to volatile organic compounds. Journal of Alloys and Compounds, 2019, 793, 24-30.	5.5	87
66	Highly sensitive ethylene sensors using Pd nanoparticles and rGO modified flower-like hierarchical porous α-Fe2O3. Sensors and Actuators B: Chemical, 2019, 290, 396-405.	7.8	49
67	In-situ growth of ordered Pd-doped ZnO nanorod arrays on ceramic tube with enhanced trimethylamine sensing performance. Applied Surface Science, 2019, 463, 348-356.	6.1	69
68	One-Step Synthesis of Au/SnO2/RGO Nanocomposites and Their VOC Sensing Properties. IEEE Nanotechnology Magazine, 2018, 17, 212-219.	2.0	144
69	A facile one-step hydrothermal synthesis of NiO/ZnO heterojunction microflowers for the enhanced formaldehyde sensing properties. Journal of Alloys and Compounds, 2018, 739, 260-269.	5.5	95
70	Highly Sensitive Ammonia Sensors Based on Ag-Decorated WO <sub>3</sub> Nanorods. IEEE Nanotechnology Magazine, 2018, 17, 1252-1258.	2.0	63
71	Highly sensitive and selective butanol sensors using the intermediate state nanocomposites converted from β-FeOOH to α-Fe2O3. Sensors and Actuators B: Chemical, 2018, 273, 543-551.	7.8	58
72	Low-temperature formaldehyde gas sensors based on NiO-SnO2 heterojunction microflowers assembled by thin porous nanosheets. Sensors and Actuators B: Chemical, 2018, 273, 418-428.	7.8	177

#	Article	IF	CITATIONS
73	Assembly of 3D flower-like NiO hierarchical architectures by 2D nanosheets: synthesis and their sensing properties to formaldehyde. RSC Advances, 2017, 7, 3540-3549.	3.6	44
74	CuO hollow microspheres self-assembled with nanobars: Synthesis and their sensing properties to formaldehyde. Vacuum, 2017, 144, 272-280.	3.5	35
75	A biocompatible and novelly-defined Al-HAP adsorption membrane for highly effective removal of fluoride from drinking water. Journal of Colloid and Interface Science, 2017, 490, 97-107.	9.4	64
76	UVâ€activated room temperature singleâ€sheet ZnO gas sensor. Micro and Nano Letters, 2017, 12, 813-817.	1.3	28
77	Trimethylamine Sensors Based on Au-Modified Hierarchical Porous Single-Crystalline ZnO Nanosheets. Sensors, 2017, 17, 1478.	3.8	97
78	Catalysis-Based Cataluminescent and Conductometric Gas Sensors: Sensing Nanomaterials, Mechanism, Applications and Perspectives. Catalysts, 2016, 6, 210.	3.5	8
79	Chlorobenzene sensor based on Pt-decorated porous single-crystalline ZnO nanosheets. Sensors and Actuators A: Physical, 2016, 252, 96-103.	4.1	42
80	Porous and single-crystalline ZnO nanobelts: fabrication with annealing precursor nanobelts, and gas-sensing and optoelectronic performance. Nanotechnology, 2016, 27, 355702.	2.6	32
81	Performance of a novelly-defined zirconium metal-organic frameworks adsorption membrane in fluoride removal. Journal of Colloid and Interface Science, 2016, 484, 162-172.	9.4	131
82	Novel volatile organic compound (VOC) sensor based on Ag-decorated porous single-crystalline ZnO nanosheets. Materials Express, 2016, 6, 191-197.	0.5	11
83	Ag/SnO2/graphene ternary nanocomposites and their sensing properties to volatile organic compounds. Journal of Alloys and Compounds, 2016, 659, 127-131.	5.5	48
84	Effective removal of fluoride by porous MgO nanoplates and its adsorption mechanism. Journal of Alloys and Compounds, 2016, 675, 292-300.	5.5	103
85	Performance of novel hydroxyapatite nanowires in treatment of fluoride contaminated water. Journal of Hazardous Materials, 2016, 303, 119-130.	12.4	134
86	Formation of Carbonized Polystyrene Sphere/hemisphere Shell Arrays by Ion Beam Irradiation and Subsequent Annealing or Chloroform Treatment. Scientific Reports, 2015, 5, 17529.	3.3	17
87	Facile preparation of size-controlled TiO2 nanoparticles by hot-filament metal oxide deposition method and their gas sensing properties to NO2. Functional Materials Letters, 2015, 08, 1550043.	1.2	1
88	CTAB-Assisted Hydrothermal Synthesis of WO3Hierarchical Porous Structures and Investigation of Their Sensing Properties. Journal of Nanomaterials, 2015, 2015, 1-10.	2.7	3
89	Sub-ppb detection of acetone using Au-modified flower-like hierarchical ZnO structures. Sensors and Actuators B: Chemical, 2015, 219, 209-217.	7.8	95
90	The risk management of virtual enterprise based on bilateral negotiation. , 2015, , .		0

#	Article	IF	CITATIONS
91	Ag-decorated ultra-thin porous single-crystalline ZnO nanosheets prepared by sunlight induced solvent reduction and their highly sensitive detection of ethanol. Sensors and Actuators B: Chemical, 2015, 209, 975-982.	7.8	87
92	Interlaced nanoflake-assembled flower-like hierarchical ZnO microspheres prepared by bisolvents and their sensing properties to ethanol. Journal of Alloys and Compounds, 2015, 632, 645-650.	5.5	56
93	New Strategy for Rapid Detection of the Simulants of Persistent Organic Pollutants Using Gas Sensor Based on 3-D Porous Single-Crystalline ZnO Nanosheets. IEEE Sensors Journal, 2015, 15, 3668-3674.	4.7	12
94	Wide pH range for fluoride removal from water by MHS-MgO/MgCO3 adsorbent: Kinetic, thermodynamic and mechanism studies. Journal of Colloid and Interface Science, 2015, 446, 194-202.	9.4	62
95	Synthesis of WO3 flower-like hierarchical architectures and their sensing properties. Journal of Alloys and Compounds, 2015, 649, 731-738.	5.5	38
96	Graphene-based hybrids for chemiresistive gas sensors. TrAC - Trends in Analytical Chemistry, 2015, 68, 37-47.	11.4	276
97	Efficient removal of fluoride by hierarchical MgO microspheres: Performance and mechanism study. Applied Surface Science, 2015, 357, 1080-1088.	6.1	60
98	Flower-like hierarchical structures consisting of porous single-crystalline ZnO nanosheets and their gas sensing properties to volatile organic compounds (VOCs). Journal of Alloys and Compounds, 2015, 626, 124-130.	5.5	99
99	Enhanced adsorption of cadmium ions by 3D sulfonated reduced graphene oxide. Chemical Engineering Journal, 2015, 262, 1292-1302.	12.7	150
100	Catalyst-free growth of one-dimensional ZnO nanostructures on SiO2 substrate and in situ investigation of their H2 sensing properties. Journal of Alloys and Compounds, 2015, 622, 73-78.	5.5	41
101	A Novel Fluorescence Nanoprobing Strategy for Fluoride Anions Detection in Water. Nanoscience and Nanotechnology Letters, 2015, 7, 546-554.	0.4	1
102	Facile synthesis of porous single crystalline ZnO nanoplates and their application in photocatalytic reduction of Cr(VI) in the presence of phenol. Journal of Hazardous Materials, 2014, 276, 400-407.	12.4	96
103	UV irradiation synthesis of an Au–graphene nanocomposite with enhanced electrochemical sensing properties. Journal of Materials Chemistry A, 2013, 1, 9189.	10.3	145
104	A three-dimensional hierarchical CdO nanostructure: Preparation and its improved gas-diffusing performance in gas sensor. Sensors and Actuators B: Chemical, 2013, 184, 260-267.	7.8	33
105	Porous TiO2 nanowires derived from nanotubes: Synthesis, characterzation and their enhanced photocatalytic properties. Microporous and Mesoporous Materials, 2013, 181, 146-153.	4.4	19
106	Synthesis of Porous Gold Based on Gold–Thiol Coordination Polymer and Its Application in SERS Detection with High Activity and High Reproducibility. Chemistry Letters, 2013, 42, 407-409.	1.3	0
107	Plasma- and anneal-assisted hybridization of SWCNT-Au network for rapid and high-sensitive electrical detection of antibody-antigen interactions. Journal of Materials Chemistry, 2012, 22, 6139.	6.7	4
108	Modification of coral-like SnO2 nanostructures with dense TiO2 nanoparticles for a self-cleaning gas sensor. Talanta, 2012, 99, 394-403.	5.5	15

#	Article	IF	CITATIONS
109	Parts per billion-level detection of benzene using SnO2/graphene nanocomposite composed of sub-6nm SnO2 nanoparticles. Analytica Chimica Acta, 2012, 736, 100-107.	5.4	84
110	Metal Oxide Nanostructures and Their Gas Sensing Properties: A Review. Sensors, 2012, 12, 2610-2631.	3.8	938
111	Novel hierarchically-packed tin dioxide sheets for fast adsorption of organic pollutant in aqueous solution. Journal of Materials Chemistry, 2012, 22, 2885-2893.	6.7	13
112	Preparation of a leaf-like CdS micro-/nanostructure and its enhanced gas-sensing properties for detecting volatile organic compounds. Journal of Materials Chemistry, 2012, 22, 17782.	6.7	82
113	SnO <sub>2</sub> /Reduced Graphene Oxide Nanocomposite for the Simultaneous Electrochemical Detection of Cadmium(II), Lead(II), Copper(II), and Mercury(II): An Interesting Favorable Mutual Interference. Journal of Physical Chemistry C, 2012, 116, 1034-1041.	3.1	431
114	Study on the interfacial structures of Tin oxide/multiwalled carbon nanotube heterojunctions. RSC Advances, 2012, 2, 1942.	3.6	6
115	Sensitive detection of indoor air contaminants using a novel gas sensor based on coral-shaped tin dioxide nanostructures. Sensors and Actuators B: Chemical, 2012, 165, 24-33.	7.8	8
116	Synthesis and gas sensing properties of hierarchical meso-macroporous SnO2 for detection of indoor air pollutants. Sensors and Actuators B: Chemical, 2012, 166-167, 519-525.	7.8	55
117	Novel hybridized SWCNT–PCD: synthesis and host–guest inclusion for electrical sensing recognition of persistent organic pollutants. Journal of Materials Chemistry, 2011, 21, 11109.	6.7	26
118	Dense doping of indium to coral-like SnO <sub>2</sub> nanostructures through a plasma-assisted strategy for sensitive and selective detection of chlorobenzene. Nanotechnology, 2011, 22, 315501.	2.6	21
119	Electronic chip based on self-oriented carbon nanotube microelectrode array to enhance the sensitivity of indoor air pollutants capacitive detection. Sensors and Actuators B: Chemical, 2011, 153, 103-109.	7.8	24
120	A novel porous anodic alumina based capacitive sensor towards trace detection of PCBs. Sensors and Actuators B: Chemical, 2011, 157, 641-646.	7.8	21
121	Synthesis of novel layer-packed In <inf>2</inf> O <inf>3</inf> nanostructures and their application in gas sensor for detecting indoor air contaminants. , 2011, , .		0
122	Electrochemistry of water in 1-butyl-3-methylimidazolium tetrafluoroborate at nickel electrode: application to hydrogen peroxide production and water sensing. Mikrochimica Acta, 2010, 168, 325-329.	5.0	1
123	Novel nanoparticle detection method using electrochemical device based on anodic aluminum oxide nanopore membrane. Procedia Engineering, 2010, 7, 100-105.	1.2	1
124	Comparison on gas-sensing properties of single- and multi-layered SnO2 nanostructures in drug-precursors detection. Procedia Engineering, 2010, 7, 123-129.	1.2	1
125	Mesoporous SnO2 sensor prepared by carbon nanotubes as template and its sensing properties to indoor air pollutants. Procedia Engineering, 2010, 7, 172-178.	1.2	13
126	p-Hexafluoroisopropanol phenyl covalently functionalized single-walled carbon nanotubes for detection of nerve agents. Carbon, 2010, 48, 1262-1270.	10.3	68

#	Article	IF	CITATIONS
127	A novel coral-like porous SnO <sub>2</sub> hollow architecture: biomimetic swallowing growth mechanism and enhanced photovoltaic property for dye-sensitized solar cell application. Chemical Communications, 2010, 46, 472-474.	4.1	120
128	Assembly, formation mechanism, and enhanced gas-sensing properties of porous and hierarchical SnO <sub>2</sub> hollow nanostructures. Journal of Materials Research, 2010, 25, 1992-2000.	2.6	8
129	Nanocomposites of sub-10 nm SnO2 nanoparticles and MWCNTs for detection of aldrin and DDT. Analytical Methods, 2010, 2, 1710.	2.7	17
130	Notice of Retraction: Survey on Pre-service Teacher Educational Technology Literacy Status: Take the Jiangxi Normal University as the Example. , 2010, , .		0
131	Novel facile detection of persistent organic pollutants using highly sensitive gas sensor. Talanta, 2010, 82, 409-416.	5.5	5
132	Novel pyrenehexafluoroisopropanol derivative-decorated single-walled carbon nanotubes for detection of nerve agents by strong hydrogen-bonding interaction. Analyst, The, 2010, 135, 368-374.	3.5	98
133	Porous Hierarchical In <sub>2</sub> O <sub>3</sub> Micro-/Nanostructures: Preparation, Formation Mechanism, and Their Application in Gas Sensors for Noxious Volatile Organic Compound Detection. Journal of Physical Chemistry C, 2010, 114, 4887-4894.	3.1	111
134	One-step synthesis of UV-induced Pt nanotrees on the surface of DNA network. Materials Research Bulletin, 2009, 44, 1270-1274.	5.2	11
135	A novel highly sensitive gas ionization sensor for ammonia detection. Sensors and Actuators A: Physical, 2009, 150, 218-223.	4.1	69
136	A novel ammonia sensor based on high density, small diameter polypyrrole nanowire arrays. Sensors and Actuators B: Chemical, 2009, 142, 204-209.	7.8	80
137	Development of sensors based on CuO-doped SnO2 hollow spheres for ppb level H2S gas sensing. Journal of Materials Science, 2009, 44, 4326-4333.	3.7	65
138	Gas sensors for ammonia detection based on polyaniline-coated multi-wall carbon nanotubes. Materials Science and Engineering B: Solid-State Materials for Advanced Technology, 2009, 163, 76-81.	3.5	108
139	Novel capacitive sensor: Fabrication from carbon nanotube arrays and sensing property characterization. Sensors and Actuators B: Chemical, 2009, 140, 396-401.	7.8	35
140	Triethylenetetramine (TETA)-assisted synthesis, dynamic growth mechanism, and photoluminescence properties of radial single-crystalline ZnS nanowire bundles. Journal of Crystal Growth, 2009, 311, 1423-1429.	1.5	21
141	Synthesis of close-packed multi-walled carbon nanotube bundles using Mo as catalyst. Carbon, 2009, 47, 1652-1658.	10.3	31
142	Morphogenesis and Crystallization of ZnS Microspheres by a Soft Templateâ€Assisted Hydrothermal Route: Synthesis, Growth Mechanism, and Oxygen Sensitivity. Chemistry - an Asian Journal, 2009, 4, 174-180.	3.3	17
143	In Situ Growth of Tin Oxide Nanowires, Nanobelts, and Nanodendrites On the Surface of Iron-Doped Tin Oxide/Multiwalled Carbon Nanotube Nanocomposites. Journal of Physical Chemistry C, 2009, 113, 20583-20588.	3.1	9
144	Nanomaterial-Assisted Signal Enhancement of Hybridization for DNA Biosensors: A Review. Sensors, 2009, 9, 7343-7364.	3.8	43

#	Article	IF	CITATIONS
145	Novel porous single-crystalline ZnO nanosheets fabricated by annealing ZnS(en) <sub>0.5</sub> (en =) Tj ETQq1 Nanotechnology, 2009, 20, 125501.	1 0.78431 2.6	4 rgBT /Ove 137
146	Preparation of Porous Tin Oxide Nanotubes Using Carbon Nanotubes as Templates and Their Gas-Sensing Properties. Journal of Physical Chemistry C, 2009, 113, 9581-9587.	3.1	91
147	Novel Single-Crystalline Hierarchical Structured ZnO Nanorods Fabricated via a Wet-Chemical Route: Combined High Gas Sensing Performance with Enhanced Optical Properties. Crystal Growth and Design, 2009, 9, 1716-1722.	3.0	67
148	Dynamic Prebreakdown Current Measurement of Nanotips-Based Gas Ionization Sensor Application at Ambient Atmosphere. IEEE Sensors Journal, 2009, 9, 435-440.	4.7	10
149	Fabrication of gas ionization sensors using well-aligned MWCNT arrays grown in porous AAO templates. Colloids and Surfaces A: Physicochemical and Engineering Aspects, 2008, 313-314, 355-358.	4.7	14
150	Template synthesis, organic gas-sensing and optical properties of hollow and porous In <sub>2</sub> O <sub>3</sub> nanospheres. Nanotechnology, 2008, 19, 345704.	2.6	106
151	A Novel Antimonyâ^'Carbon Nanotubeâ^'Tin Oxide Thin Film:  Carbon Nanotubes as Growth Guider and Energy Buffer. Application for Indoor Air Pollutants Gas Sensor. Journal of Physical Chemistry C, 2008, 112, 6119-6125.	3.1	54
152	Detection of volatile organic compounds by using a single temperature-modulated SnO2gas sensor and artificial neural network. Smart Materials and Structures, 2007, 16, 701-705.	3.5	27
153	In situ fabrication of carbon nanotube/nanofibres from the bulk polymer at mild temperature. Materials Letters, 2006, 60, 2312-2314.	2.6	0
154	DYNAMIC CHARACTERISTICS OF SnO2 GAS SENSOR FOR LPG DETECTION. International Journal of Information Acquisition, 2004, 01, 225-230.	0.2	0
155	Carboxylation multi-walled carbon nanotubes modified with LiClO4for water vapour detection. Nanotechnology, 2004, 15, 1284-1288.	2.6	43
156	Quantitative analysis of pesticide residue based on the dynamic response of a single SnO2 gas sensor. Sensors and Actuators B: Chemical, 2004, 99, 330-335.	7.8	28
157	Gas sensing behavior of a single tin dioxide sensor under dynamic temperature modulation. Sensors and Actuators B: Chemical, 2004, 99, 444-450.	7.8	98
158	New approach for the detection of organophosphorus pesticide in cabbage using SPME/SnO2 gas sensor: principle and preliminary experiment. Sensors and Actuators B: Chemical, 2004, 102, 235-240.	7.8	12
159	New approach for the detection of organophosphorus pesticide in cabbage using SPME/SnO2 gas sensor: principle and preliminary experiment. Sensors and Actuators B: Chemical, 2004, 102, 235-235.	7.8	2
160	Study of Influencing Factors of Dynamic Measurements Based on SnO2 Gas Sensor. Sensors, 2004, 4, 95-104.	3.8	42
161	Rapid detection of hazardous gas using one SnO/sub 2/ gas sensor based on dynamic measurement. , 0, ,		2